Preparation, Characterization, and Properties of Mixed Organic and Polymeric Self-Assembled Multilayers

DeQuan Li,*,† M. Lütt,‡ M. R. Fitzsimmons,‡ R. Synowicki,§ M. E. Hawley,|| and G. W. Brown||

Contribution from the Chemical Science and Technology Division, Manuel Lujan Jr. Neutron Scattering Center, and Materials Science and Technology Division, Los Alamos National Laboratory, Los Alamos, New Mexico 87545, and J. A. Woollam Co., Inc., 650 J Street, Suite 39, Lincoln, Nebraska 68508

Received April 13, 1998

Abstract: Multilayer thin films consisting of layer-pairs of oppositely charged macrocycles (nickel phthalocyanine tetrasulfonate, NiPc) and macromolecules (poly(diallydimethylammonium) chloride, PDDA) were fabricated using self-assembly techniques. The film structures were characterized with X-ray reflectometry, from which the roughness (∼2−7 Å) of the film growth surface, the average electron density of each layer-pair, the mean thickness of the layer-pairs (∼10.5 Å), and the overall thickness of the multilayer samples were deduced. Measurements of film thicknesses were applied as constraints to an analysis of spectroscopic ellipsometry measurements of the films. Imposition of these constraints increased the confidence of the optical constant refinements deduced from ellipsometry. We find, for multilayers of PDDA and NiPc, a refractive index of $n \approx 1.6-1.8$ in the nonabsorption region of the visible and near-infrared (IR) spectrum and an extinction coefficient in close agreement with the measured electron optical absorption at 630 and 665 nm. Atomic force microscopy was also used to observe surface morphology and determine grain size distribution and roughness for selected films. An increase in surface roughness (∼5−15 Å) was observed as the number of layer-pairs in the film increased from 3 to 27.

Introduction

Fabrication of multilayer thin films is becoming increasingly important in applications using optical waveguides and other integrated optical devices, for example, display devices, since unusual optical phenomena occurring at the interfaces in multilayered structures can be exploited for these applications.[1−5] In contrast to monolayer films,[6−12] the structures, chemistry, and electronic properties of interfaces, which give rise to desirable optical behavior, also complicate the fabrication of multilayered structures. For example, strain across internal interfaces, chemical interactions, and electronic properties, for example, compatibility of work functions, at the multilayer interfaces must be optimized in order to maintain structural regularity and integrity.

The multilayered structures are typically grown on inorganic oxide surfaces. These surfaces are usually terminated with hydroxyl groups (e.g., silica,[13,14] which has approximately five hydroxyl groups per nm^2). Disassociation or replacement of the hydroxyl proton will cause the surface to become slightly negatively charged. The surface charge density is affected by a variety of factors including temperature, pH in solution, and other chemical elements present in or on the substrate surface. For example, at 25 °C and pH = 8, the surface charge density of silica is about 0.24 charges per nm^2.[15] These negatively charged surface sites do not interact strongly with monovalent cations but do serve as anchor sites for covalently bound polycations or large charged clusters; therefore, charged-ordered thin films can be fabricated by taking advantage of the slightly negatively charged surface sites by first depositing a positively charged organic material.

Molecular self-assembly that exploits charge attraction between oppositely charged materials is used to fabricate multilayered structures in a layer-by-layer manner.[16−22] From a processing point-of-view, molecular self-assembly is interesting,

† Chemical Science and Technology Division, Los Alamos National Laboratory.
‡ Manuel Lujan Jr. Neutron Scattering Center.
§ J. A. Woollam Co., Inc.
|| Materials Science and Technology Division, Los Alamos National Laboratory.

(1) Knoll, W. *Pure Appl. Chem.* **1995**, *67* (1), 87−94.
(2) Hayashi, T.; Maruno, T.; Yamashita, A.; Folsch, S.; Kanbara, H.; Konami, H.; Hatano, M. *Jpn. J Appl. Phys., Part 1* **1995**, *34* (7b), 3884−3888.
(3) Li, D. Q.; Ratner, M. A.; Marks, T. J.; Zhang, C. H.; Yang, J.; Wong, G. K. *J. Am. Chem. Soc.* **1990**, *112*, 7389.
(4) Yang, X.; McBranch, D.; Swanson, B.; Li, D. Q. *Angew. Chem., Int. Ed. Engl.* **1996**, *35*, 538.
(5) Takada, N.; Tsutsui, T.; Saito, S. *Appl. Phys. Lett.* **1993**, *63* (15), 2032−2034.
(6) Labinis, P. E.; Hickman, J. J.; Wrighton, M. S.; Whiteside, G. M. *Science (Washingtion, D.C.)* **1989**, *245*, 845.
(7) Strong, L.; Whiteside, G. M. *Langmuir* **1988**, *4*, 546.
(8) Pale-Grosdemange, C.; Simon, E. S.; Prime, K. L.; Whitesides, G. M. *J. Am. Chem. Soc.* **1991**, *113*, 12.
(9) Nuzzo, R. G.; Dubois, L. H.; Allara, D. L. *J. Am. Chem. Soc.* **1990**, *112*, 558.
(10) Bryant, M. A.; Pemberton, J. E. *J. Am. Chem. Soc.* **1991**, *113*, 8284.
(11) Porter, M. D.; Bright, T. B.; Allara, D. L.; Chidsey, C. E. D. *J. Am. Chem. Soc.* **1987**, *109*, 3559.
(12) Moore, L. W.; Springer, K. N.; Shi, J. X.; Yang, X.; Swanson, B. I.; Li, D. Q. *Adv. Mater.* **1995**, *7*, 729.
(13) Gun, J.; Iscovici, R.; Sagiv, J. *J. Colloid Interface Sci.* **1984**, *101*, 201−213.
(14) Zhuravlev, L. T. *Langmuir* **1987**, *3*, 316−318.
(15) Brady, P. V.; Walther, J. V. *Am. J. Sci.* **1992**, *292* (9) 639−658.
(16) Decher, G.; Hong, J.-D. *Ber. Bunsen-Ges. Phys. Chem.* **1991**, *95*, 1430−1434.

S0002-7863(98)01232-3 CCC: $15.00
Published on Web 08/15/1998

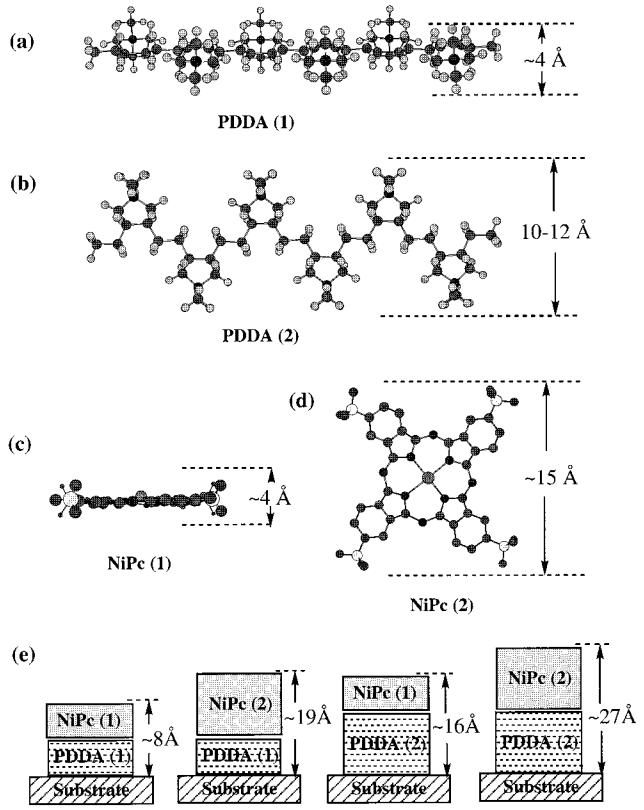

Figure 1. The idealized linear structure of PDDA lying flat or PDDA-(1) gives a thickness of ~4 Å (a). The idealized linear structure of PDDA standing up or PDDA(2) yields a higher thickness value of ~10−12 Å (b). The structure of NiPc lying flat or NiPc(1) gives a thickness of ~4 Å (c). The structure of NiPc standing on edge or NiPc-(2) yields a higher thickness value of ~15 Å (d). Four idealized layer-pair combinations between PDDA and NiPc yield ~8, 16, 19, and 27 Å thickness values, respectively (e).

because the technique is readily adapted for automated fabrication; however, the technique relies upon charge−charge interactions, which are weaker than covalent bonds. In some cases, the mechanical and chemical robustness of multilayered structures fabricated with molecular self-assembly can be an issue if, for example, the structures were used in devices exposed to a changing environment.

In this manuscript, a process for fabricating mechanically and chemically robust positively charged poly(diallydimethylammonium) chloride (PDDA) and negatively charged nickel phthalocyanine (NiPc) thin-film structures grown directly on transparent silica substrates using molecular self-assembly is described (Figure 1). To gauge the success of thin-film formation, X-ray reflectometry, atomic force microscopy (AFM), optical electronic absorption, and spectroscopic ellipsometry were used to characterize the PDDA−NiPc system. Small-angle X-ray reflectometry provides information about the electron density profile and thickness of the multilayer and the roughness of the growth interface. AFM explores surface topology and surface roughness. Optical absorption gives information about the molecular orientation and amount of materials in the sample. Finally, spectroscopic ellipsometry gives the complex dielectric function of the film, provided its thickness is known (in this work film thickness was measured using X-ray reflectometry). Characterization of the linear optical components of the dielectric function, that is, the refractive index n and the extinction coefficient k, can be done with a high degree of confidence when information obtained from reflectometry and ellipsometry is combined. This characterization serves as a foundation for later understanding of the nonlinear optical behavior of the multilayered structures.

Experimental Section

Materials. The chemicals were purchased from Aldrich and used without further treatment. PDDA was obtained as 20 wt % in water solution. All dipping solutions were prepared with deionized water. Glass substrates—microscope slides for both X-ray and ellipsometry measurements—were obtained from Fisher Scientific or VWR Scientific. X-ray reflectivity measurements were carried out with both thick (1 cm) and thin (0.5 mm) silicon wafers (Siltec Silicon).

Preparation of Self-Assembled Multilayers. Silica substrates were cleaned using a detergent solution in an ultrasonic cleaner and rinsed in deionized water. After being rinsed, the substrates were immersed in the positively charged PDDA polymer at a 10 mM concentration for about 5 min. Because positively charged polymers are attracted to the negatively charged substrate surfaces, a monolayer of PDDA will spontaneously disperse on the substrates. Next, the coated substrates were washed with deionized water five times to ensure that all the nonadsorbed materials were removed. The PDDA-coated substrates were immersed in a 1 mM aqueous solution of NiPc for 5 min, which was followed by again rinsing with deionized water five times. After one dipping cycle, consisting of one dip in PDDA followed by one dip in the NiPc solution, a layer-pair of PDDA and NiPc was formed on the substrate surface. Additional layer-pairs were deposited to form a multilayer, since the negatively charged NiPc surface attracts PDDA and vice versa (Figure 1). Three samples consisting of 3, 9, and 27 layer-pairs were fabricated for both the X-ray reflectometry and spectroscopic ellipsometry studies. Many other samples with different numbers of deposited layer-pairs were prepared for optical absorption studies.

X-ray Reflectometry Measurements. X-ray reflectometry involves measuring the intensity of the X-ray beam specularly reflected by planar interfaces in a sample relative to the intensity of the incident X-ray beam illuminating the sample. X-rays with a wavelength of $\lambda = 1.54$ Å were selected using a graphite monochromator from a white spectrum produced by an 18 kW rotating Cu anode X-ray generator. The X-ray beam was collimated by a pair of slits between the monochromator and sample. The intensity of the incident X-ray beam was monitored using a scintillation detector and a Mylar sheet, which scattered a small portion of the beam into the detector. Measurement of the intensity of the incident X-ray beam was required in order to know the exposure of the sample to the beam. The X-ray beam impinges onto the sample at a glancing angle, θ (typically 1°), which is the angle between the incident beam and its projection on the sample surface. The intensity of the X-ray beam specularly reflected by the sample was measured with a position sensitive detector (PSD) located 490 mm from the sample. The recorded intensity was a Gaussian-shaped peak. The specular reflectivity is the integral of the peak after removal of the instrumental background, which is measured in a region of the PSD well away from the position of the reflected beam peak. A reflectivity profile is a collection of reflectivity measurements made for different values of momentum transfer Q_z, where $Q_z = 4\pi \sin(\theta)/\lambda$.

Atomic Force Microscopy. The surface roughness of 3-, 9-, and 27-layer-pair films was determined from atomic force microscopy data obtained with a Digital Instruments Nanoscope III multimode probe. Because of the softness of the deposited material, imaging was done with a 200 μm long silicon cantilever (spring constant $\approx$ 0.12 N/m and resonant frequency $\approx$ 180 kHz) used in noncontact tapping mode. No modification of the surface was observed after repeated scanning.

(17) Sun, Y.; Zhang, X.; Sun, C.; Wang, Z.; Shen, J.; Wang, D.; Li, T. *J. Chem. Soc., Chem. Commun.* **1996**, 2379−2380.
(18) Schmitt, J.; Grunewald, T.; Kjar, K.; Pershan, P.; Decher, G.; Losche, M. *Macromolecules* **1993**, *26*, 7058−7063.
(19) Lee, J. K.; Yoo, D. S.; Handy, E. S.; Rubner, M. F. *Appl. Phys. Lett.* **1996**, *69*, 1686−1688.
(20) Ariga, K.; Lvov, Y.; Kunitake, T. *J. Am. Chem. Soc.* **1997**, *119*, 224−2231.
(21) Knoll, W. *Curr. Opin. Colloid Interface Sci.* **1996**, *1*, 137−143.
(22) Decher, G. *Science* **1997**, *277*, 1232−1237.

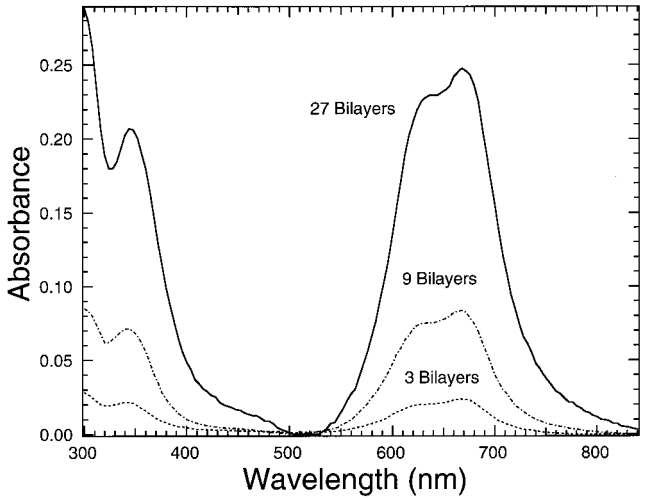

Figure 2. Optical absorption of 3 layer-pairs of PDDA−NiPc (dashed), 9 layer-pairs of PDDA−NiPc (dash−dot), and 27 layer-pairs of PDDA−NiPc (solid). The α and β absorptions at 630 and 665 nm are due to the $\pi-\pi^*$ electronic transitions in NiPc molecules.

A dual-mode technique was used to acquire both surface height maps in the standard feedback mode and pseudoderivatives of surface topography through an amplitude imaging mode. The amplitude images allow better visualization of the grain structure by removing long-range variations and offsets. Surface height images were used for all calculations. Root-mean-square surface roughness was calculated with the software supplied by the instrument manufacturer, and grain size distributions were generated with NIH Image. A minimum grain size cutoff of 1500 nm^2 was chosen based on visual assessment of the amplitude images.

Ellipsometry Measurements. The self-assembled thin films were characterized with a J. A. Woollam Company variable angle spectroscopic ellipsometer (VASE) system. The back sides of the glass sample substrates were roughened to suppress reflections from these surfaces. The ellipsometric parameters ψ and Δ, which are related to the ellipticity of the polarized light, were acquired at fixed angles between the light and the sample surface normal (55, 65, and 75°, respectively) and analyzed using the WVASE32 software package. VASE data were fit over the spectral region of 290−1200 nm. The data sets were analyzed using fixed layer thicknesses deduced for the multilayer samples from the X-ray reflectometry study. This allowed determination of the optical constants for each film without the need for an additional fitted parameter. The optical constants of the glass substrate were determined separately and were not allowed to vary during the data fits on the organic multilayers. The optical constants for three organic films were determined with direct and parametrized models (see discussion section).

Results

In an aqueous solution, PDDA will form a uniform, nanometer-thick thin film on a silica substrate, because PDDA is attracted to the negatively charged substrate surface. A negatively charged NiPc macrocycle will bind to the dispersed positively charged polymeric PDDA monolayer. Multilayer thin films were obtained by alternately dipping the sample in solutions of PDDA and NiPc. The growth of these films was monitored by measuring the absorption of 630 and 665 nm light (Figure 2).

The reflectivity profiles, normalized to unit reflectivity, are shown as a function of momentum transfer Q_z for the three samples with $N = 3$, 9, and 27 (Figure 3). The maximum of the reflectivity profile occurs at a value of Q_z corresponding to the condition when the X-ray radiation in the sample is evanescent ($Q_z < Q_c$),[23] and the sample surface subtends the full width of the X-ray beam. The oscillation in the reflectivity

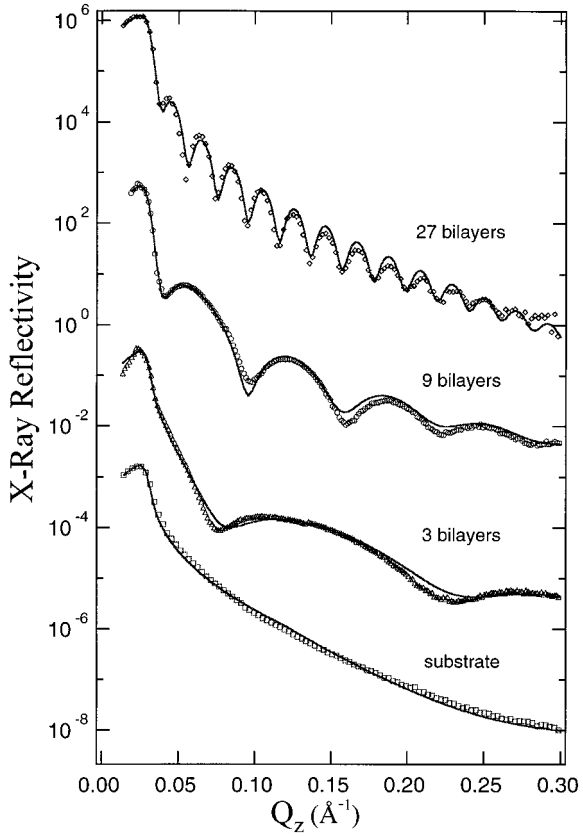

Figure 3. X-ray reflectivity profiles of the glass substrate (squares), 3 layer-pairs of PDDA−NiPc (triangles), 9 layer-pairs of PDDA−NiPc (circles), and 27 layer-pairs of PDDA−NiPc (diamonds). Solid lines are fits from the calculated model, which yields the thickness (t), roughness (δ), and electron density (ρ). The curves are displaced for the sake of clarity.

profiles with Q_z is caused by interference between the X-ray beams reflected by the film−air and film−substrate interfaces. The frequency of the oscillation is inversely related to the film thickness.

Ellipsometry measurements of the samples were made for a variety of incident angles (55, 65, and 75°). The measured data are called the ellipsometric parameters Ψ and Δ, which are related to the ellipticity of the reflected light. The ellipsometric parameters for the 27-layer-pair sample measured from 300 to 1300 nm are shown in Figure 4. The major features in the Ψ and Δ parameters are due to the α and β absorption bands in the NiPc molecules. In the nonresonant regions, both Ψ and Δ are fairly featureless.

Discussion

Formation of Nanometer-Thick Polymeric Films on Oxide Surfaces. Oxide surfaces have a low negative charge density and can be used to anchor polycations rather than monovalent cations because charge−charge attractions are weak in water. For example, the energy to pull apart an ion pair at a distance of 5 Å is about 3.5 kJ/mol; therefore, a single charge interaction is usually not strong enough to produce well-organized structures. Multiple charge attractions, however, are able to generate good surface adhesion between films and substrates. PDDA and NiPc have been chosen for this study because PDDA is a hard polycation and the absorption of NiPc onto PDDA-coated surfaces can be easily monitored with ultraviolet and visible (UV−vis) spectroscopy.

(23) Parratt, L. G. *Phys. Rev.* **1954**, *95*, 359.

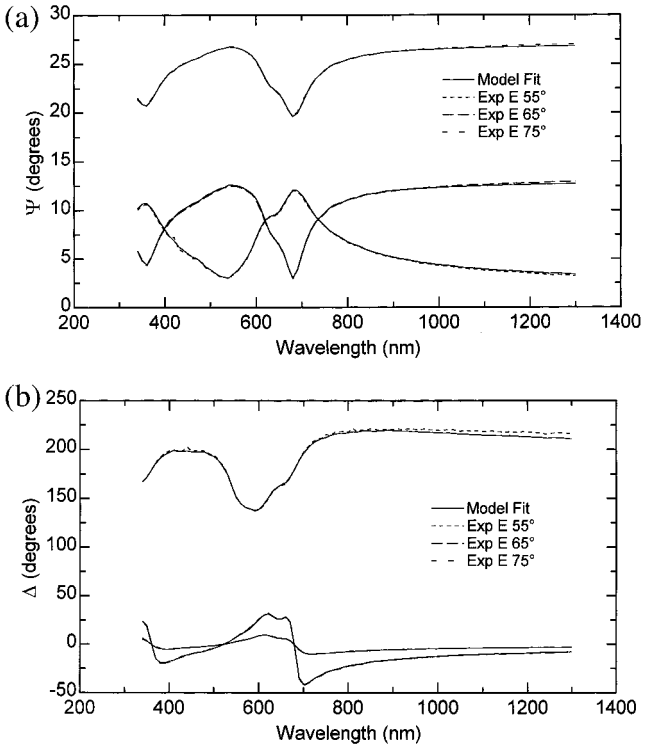

Figure 4. Measured ellipsometric parameters Ψ (a) and Δ (b) on 27 layer-pairs of PDDA−NiPc are shown as a function of the wavelength at incident angles of 55° (dashed lines), 65° (long dashed lines), and 75° (dashed broken lines) along with theoretical fits from the parametrized model (solid lines).

In an aqueous solution, the most favorable configuration of PDDA should be a zigzag structure (Figure 1 parts a and b) with the positive ammonium charges at maximum distance from each other, since an interaction between these charges is repulsive. PDDA can be packed on the oxide surface in one of two ways—either the zigzag structure (Figure 1a) can lie flat on the substrate with a thickness of ∼4 Å or the zigzag structure may stand up (Figure 1b) producing a film with a larger thickness of ∼10−12 Å. NiPc macrocycles can also be arranged in one of two packing structures—one lying flat with a minimum thickness of ∼4 Å (Figure 1c) and the other standing on edge with a thickness of ∼15 Å (Figure 1d). The total number of unique arrangements for PDDA and NiPc will be four with thicknesses of ∼8, 16, 19, and 27 Å (Figure 1e). The layer-pair thickness observed previously for NiPc and PDDA was ∼10 Å,[24] which suggests that both PDDA and NiPc adopt the flat configuration (Figure 1 parts a and c). However, one exception was noted previously—the thickness of the first deposited PDDA and NiPc layers on *silicon*[24] was consistent with a structure in which PDDA and NiPc stood up (Figure 1 parts b and d).

On the basis of an earlier study[24] and the sign of the surface charge density, the first polymeric layer that attaches to the oxide substrate surface is PDDA. This material provides many positively charged surface sites, which serve as a bridge for binding the next (NiPc) layer. After one dipping cycle, consisting of one dip in PDDA followed by one dip in the NiPc solution, a layer-pair consisting of PDDA and NiPc was formed on the substrate surface; thin films consisting of multiple layer-pairs were fabricated by repeating the above sequential dipping cycle in PDDA and NiPc. The multilayer fabrication procedure has been automated, and thin films with selected properties and chemical compositions have been grown with the ease of computer control, though the samples reported here were made by hand.

X-ray Reflectometry. The X-ray reflectivity of a thin film depends on the variation of the electron scattering density as a function of the depth into the film averaged over its lateral dimensions. Typically, a reflectivity profile (see, for example, Figure 3) is related to the squared modulus of the Fourier transform of the variation in the electron density profile through the Fresnel reflectivity.[25] More simply, the interference between electromagnetic waves reflected by planar interfaces is calculated with the Parratt formalism. Using this formalism, the sample is considered to consist of layers of materials with electron densities ρ_i and thicknesses Δ_i. A difference, or contrast, between the electron densities of the *i*th layer and those of its neighbors produces fringes or oscillations in the sample reflectivity. The amplitude of the fringes (see, for example, Figure 3) is related to the magnitude of the contrast, while the frequency of the fringes is a measure of sample thickness. In addition to the decay in the reflectivity of the sample with Q_z due to the Fresnel reflectivity, the reflectivity profile may be further attenuated by roughness at the interfaces. This decay is related to the variation in the displacement of the interface about the mean value from point to point across the sample in the direction along the sample surface normal. The fluctuation in interface height forms a distribution whose root-mean-square width, σ_i, increases with the attenuation of the reflectivity profile with Q_z.

The calculated reflectivity profiles for a model structure represented by ρ_e (the average electron density of PDDA and NiPc), Δ (the thickness of the multilayer sample), and σ (the roughness of the growth surface) are shown as the solid curves in Figure 3. The parameters of the model, ρ_e, Δ, and σ, from which $\rho(z)$ was determined by perturbing the values from initial guesses until the difference between the observed data (○ in Figure 3) and the fitted profile was minimized.

The fitting procedure first involved determining the electron density and roughness of the glass substrate from a measurement with no deposited film. These values were determined to be $\rho = 0.59 \pm 0.05$ e/Å^3 and $\sigma = 2.0 \pm 0.2$ Å and were held fixed in subsequent fits of thin-film models to the profiles for $N = 3$, 9, and 27. Deposition of PDDA onto the substrate is not expected to alter the composition of the substrates or the roughness of substrate surfaces. The roughness of the film−air interface after depositions of $N = 3$, 9, and 27 layer-pairs was found to be $\sigma = 2(1)$, 7(1), and 5(1) Å, respectively. More importantly for the purpose of this study, which is to report the optical constants of the films, the thicknesses of the $N = 3$-, 9-, and 27-layer-pair samples were determined to be 32(1), 95(1), and 284(1) Å, respectively.

In contrast to our earlier report, where the thickness of layer-pairs deposited onto Si substrates was large for small N values (see Figure 1 parts b and d) and approached an asymptote of 8 Å for $N > 20$ (see Figure 1 parts a and c), the thickness of a layer-pair deposited on the silica substrate in the present study was always about 11(1) Å. The lack of variability in the thicknesses for layer-pairs grown on silica substrates compared to those grown on Si substrates suggests that an interaction between the substrate surface and the deposited layer-pairs may be more important for Si substrates than for silica substrates.

Thin Film Growth Characteristics. Since NiPc has extended conjugated π electrons forming a cyclic tetrapyrrole

(24) Lütt, M.; Fitzsimmons, M.; Li, D. Q. *J. Phys. Chem. B* **1998**, *102* (2), 400−405.

(25) Parratt, L. G. *Phys. Rev.* **1954**, *95*, 359.

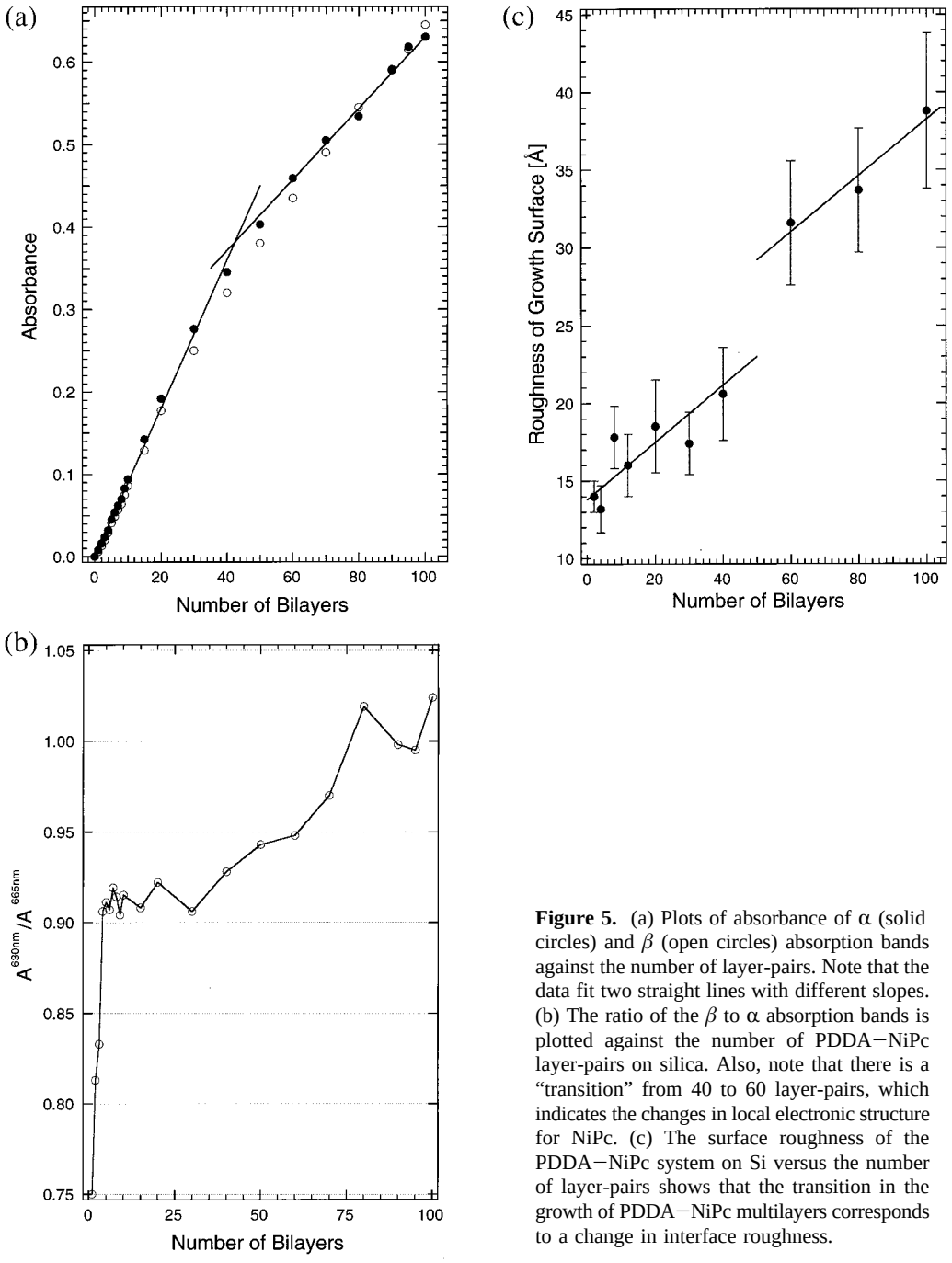

Figure 5. (a) Plots of absorbance of α (solid circles) and β (open circles) absorption bands against the number of layer-pairs. Note that the data fit two straight lines with different slopes. (b) The ratio of the β to α absorption bands is plotted against the number of PDDA−NiPc layer-pairs on silica. Also, note that there is a "transition" from 40 to 60 layer-pairs, which indicates the changes in local electronic structure for NiPc. (c) The surface roughness of the PDDA−NiPc system on Si versus the number of layer-pairs shows that the transition in the growth of PDDA−NiPc multilayers corresponds to a change in interface roughness.

structure, a film containing this compound will have α- and β-absorption bands at 630 and 665 nm (Figure 2). These absorption bands can be used to monitor the changes in electronic properties or the local solid-state environment. Figure 5a shows a measurement of the optical absorption as a function of the number of layer-pairs. For samples with $N < 50$, the absorbance of the α (630 nm, ○ symbols) and β bands (665 nm, ● symbols) increases linearly suggesting that each layer-pair deposition placed the same amount of material onto the thin film. This result is consistent with the conclusion drawn from the X-ray reflectometry study where the average thickness of each layer-pair was 11(1) Å for $N = 3$, 9, and 27. A linear increase in both absorption and thickness may further indicate that local structures of PDDA and NiPc molecules do not change for depositions numbering fewer than 50.

For $N > 50$, the absorbance also increased linearly, although with a smaller slope. In other words, the same amount of material was deposited during each dipping for depositions exceeding 50 dippings, but the amount of deposited material was less than that deposited during the first 50 dippings. Alternatively, NiPc may have adopted a different packing structure that lowered the absorption of the film. Although thick NiPc−PDDA multilayer films were grown, the transition in the growth of the sample for $N \approx 50$ suggests the occurrence of changes in growth morphology, growth mechanism, or molecular orientation, which might affect the optical properties of the film and growth of even thicker films.

A transition concomitant with morphological changes may produce a perturbation of the local electronic structures of the molecules because of alteration in the solid-state environment. The ratio of the electronic transitions for the bands at 630 and 665 nm, which monitor the difference between these two optical excitations, is plotted in Figure 5b. For the first four layer-pairs, there is an adjustment of the electronic structures due to

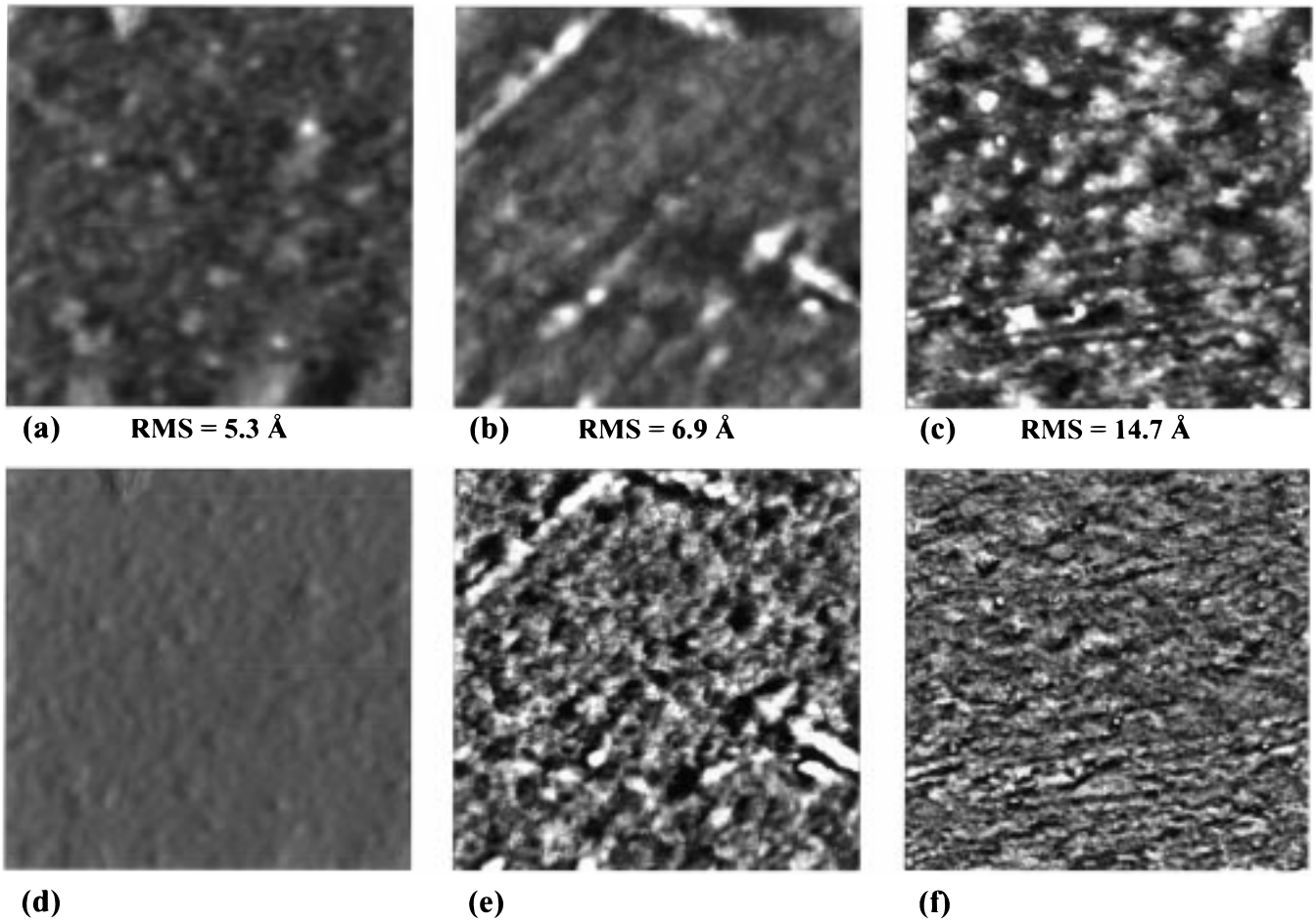

Figure 6. 1 μm × 1 μm AFM images of the surfaces of 3-, 9-, and 27-layer-pair films. Images a−c are topographs of the surface structure for 3, 9, and 27 layer-pairs; images d−f are simultaneously taken amplitude images of the same films, respectively. The latter images are pseudoderivatives of the structural data, used to emphasize fine structural information.

the influence of the newly created inorganic−organic interface. After five layer-pairs, this ratio stabilizes at ∼0.900−0.925, which suggests films of up to 40 layer-pairs will have approximately the same electronic structures for the NiPc. Between 40 and 80 layer-pairs, the absorbance ratio increases to ∼1.0. The variation in this ratio from 0.9 to 1.0 is large, suggesting less well-defined electronic structures for NiPc molecules after 50 dippings.

Interestingly, an examination of the roughness of the growth surfaces deduced that PDDA−NiPc layer-pairs deposited onto Si substrates from an earlier study[24] exhibited a discontinuity occurring between $N = 40$ and 60 like that observed in the slopes of the absorbance data for films grown on silica (Figure 5c). The increase in roughness is indicative of changes in the topology of the growth surface, which may produce a new thin-film structure. This effect was not believed to be related to the sample substrate, since the observed discontinuities in the absorbance and fitted roughness parameters from the earlier study were observations of films grown on different substrates. These observations further illustrate the complexity involved in multilayer film growth, complicated by changes perhaps in the surface wetting properties or roughness during film growth.

On the basis of these results, we also used AFM to examine the roughness of films on the surfaces of silica. Surface topography and amplitude images of 3-, 9-, and 27-layer-pair films are shown in Figure 6. While the film thicknesses increase from 3 layer-pairs to 9 and 27 layer-pairs, rms roughnesses also increase from 5.3 to 6.9 and 14.7 Å. These values are about a factor of 2 higher than the X-ray results for silica substrates. On silicon substrates, X-ray reflectivity has yielded larger roughness values for these thin films (Figure 5c). The difference in measured roughness between AFM and X-ray reflectivity is expected because AFM uses a tip to probe the surface while X-ray reflectivity employs light to measure surface roughness.

Since the NiPc molecule is a disk-shaped object with a diameter of 21 Å and thickness of ∼4 Å (Figure 1 parts c and d) and the thickness of a layer-pair of PDDA and NiPc is 11(1) Å, as determined by X-ray reflectometry, the NiPc molecules are likely to lie flat on the substrate or film surface. To test this hypothesis, changes in the absorbance of the thin films were examined as a function of the incident angle, ϕ. The absorbance of the 100-layer-pair sample is shown in Figure 7. The solid squares are measured absorbance values at ϕ incident angle normalized to the value of zero incident angle. The solid line is derived from a simple model that assumed the NiPc molecules to lie perfectly parallel to the substrate surface. For a disklike molecule with 4-fold symmetry (C_4), the following equation gives the absorbance ratio of a given optical absorption band:

$$\frac{A^{\phi}}{A^{0}} = \frac{1 + \cos^2 \phi}{2 \cos \phi} \tag{1}$$

A^0 is the absorption at 0° incidence, and A^{ϕ} is the absorption at an incident angle of ϕ. The agreement between the observed absorbance and the calculated values is good for most angles of incidence, an observation which is consistent with the

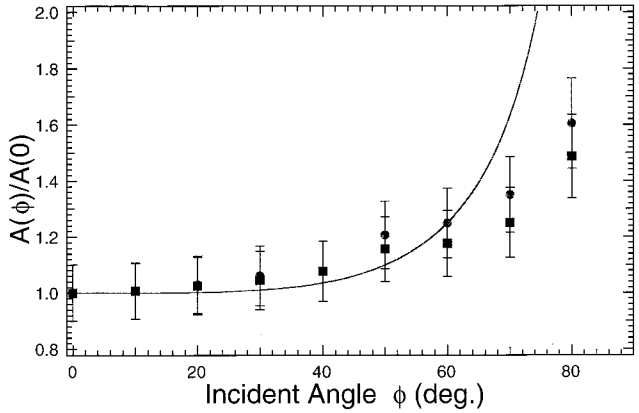

Figure 7. The ratio of absorbance from UV−vis spectroscopy at incident angle ϕ versus the absorbance at normal incidence (0°) is plotted against the incident angle (squares, $\lambda_{max} = 665$ nm; circles, $\lambda_{max} = 630$ nm). The solid line is a fit from a model assuming that NiPc is perfectly parallel to the surface.

hypothesis that the NiPc molecules are mostly parallel to the substrate surface. At higher incident angles, however, discrepancies between the calculated values and experimental values were observed. These discrepancies can be accounted for by tilting NiPc molecules from the flat orientation (Figure 1c).

Spectroscopic Ellipsometry. Spectroscopic ellipsometry measures changes in the polarization of light reflected from a sample at oblique incidence.[26−28] The change in polarization is due to the optical properties of the substrate and film overlayers, the thickness of the films, and microstructural features of the sample such as surface or interfacial roughness. The polarization change at a given wavelength and angle of incidence is given by

$$\rho = \frac{r_p}{r_s} = \tan \Psi \exp(i\Delta) \qquad (2)$$

where r_p and r_s are the complex Fresnel reflection coefficients for vector components of the light beams parallel (p) and perpendicular (s) to the plane of incidence.[29−31] The ellipsometric parameters Ψ and Δ are measured at a variety of wavelengths and incident angles from which the optical constants (n and k) of the films or substrates can be deduced.

(a) Direct Method in Ellipsometric Data Analysis. With the layer thickness held constant in the model, the two unknowns to be determined are the optical constants n and k at each wavelength. The simplest approach to determining the optical constants is to directly invert the experimental Ψ and Δ data to obtain n and k as a function of wavelength. Since interfacial roughness can affect the polarization of the light beam, the values of n and k determined using the direct method do not necessarily represent the intrinsic optical properties of the film. Optical constants determined in this way are referred to as "pseudo-optical constants" (pseudo-n and pseudo-k) because they represent the effective optical constants of the entire film including microstructure effects and not the "true" optical constants of the material.

A drawback of "direct method" data fits is that measurement noise can also perturb the deduced optical constants, since the values of n and k determined at a given wavelength are completely independent of those determined at another wavelength. Noise is especially troublesome for data taken from very thin films, since the light beam travels through less material. However, an advantage of the direct inversion method is that a model for n and k is not required. For example, subtle structure in the optical constant spectra can be clearly discerned from the data (provided the data are not noisy), which may not be discerned from a model-fitting procedure, since a model may oversimplify the real system.

(b) Parametrized Model in Ellipsometric Data Analysis. The optical constants of the organic films were also modeled using mathematical functions (dispersion models) to describe the refractive index, $n(\lambda)$, and extinction coefficient, $k(\lambda)$, of the films. In this approach, parameters of a model describing $n(\lambda)$ and $k(\lambda)$ are perturbed until a measure of error between the observed data and the fitted spectrum is minimized. As in any model-fitting algorithm, the correlation between fitted parameters and the optimization of the parameters to a false (local) minimum rather than the global minimum are concerns. To minimize these concerns, the thickness of the multilayer (often a fitted parameter in spectroscopic ellipsometry) was constrained by the values determined by X-ray reflectometry for the samples. This constraint enhances the confidence in the refinement of the parametrized model.

The organic film optical constants were modeled using an equal mixture of a standard (three-term) Cauchy relation[32] and an ensemble of three to five Lorentz oscillators—a Bruggeman effective medium approximation (EMA).[33] The standard Cauchy dispersion relation, which works well for modeling the transparent regions of the spectrum, is defined as follows:

$$n(\lambda) = A + B/\lambda^2 + C/\lambda^4 \qquad (3)$$

where A, B, and C are fit coefficients and λ is the wavelength in micrometers.

Absorption was modeled using Lorentz oscillators.[34,35] Each Lorentz oscillator is defined as a function of photon energy as follows:

$$\tilde{\epsilon}(E) = \tilde{n}^2(E) = \epsilon(\infty) + \sum_n \frac{A_n}{E^2 - {E_n}^2 + i\Gamma_n E'} \qquad (4)$$

where $\epsilon(E) = (n + ik)^2$ is the complex dielectric function. The fitted parameters in this expression are the dielectric function at infinite energies $\epsilon(\infty)$ and the amplitude (A_n), center energy (E_n), and broadening (Γ_n) of each oscillator.

One advantage of the Lorentz model is that the Kramers−Kronig (KK) relation is required between the real and imaginary parts of the refractive index (n and k), which imposes further physical requirements on the model solutions. An additional

(26) Kim, Y. D.; Cooper, S. L.; Klein, M. V.; Jonker, B. T.; *Phys. Rev. B: Condens. Matter* **1994**, *49*, 1732−1742.
(27) Kim, Y. T.; An, I. *Anal. Chem.* **1998**, *70*, 1346−1351.
(28) Guiseppielie, A.; Pradhan, S. R., Wilson, A. M.; Allara, D. I.; Zhang, P.; Collins, R. W.; Kim, Y. T. *Chem. Mater.* **1993**, *5*, 1474−1480.
(29) Aspnes, D. E. The Accurate Determination of Optical Properties by Ellipsometry. In *Handbook of Optical Constants of Solids*; Palik, E. D., Ed.; Academic Press: New York, 1985.
(30) Woollam, J. A.; Snyder, P. G. Variable Angle Spectroscopic Ellipsometry, VASE. In *Encyclopedia of Materials Characterization*; Brundle, R. C., Evans, C. A., Jr., Wilson, S., Eds.; Butterworth-Heineman: Boston, MA, 1992.
(31) Azzam, R. M. A.; Bashara, N. M. *Ellipsometry and Polarized Light*; North-Holland Publishing: New York, 1977.
(32) Pelletier, E. Methods for Determining Optical Parameters of Thin Films. In *Handbook of Optical Constants of Solids II*. Palik, E. D., Ed.; Academic Press: New York, 1991.
(33) Aspnes, D. E.; Theeten, J. B.; Hottier, F. *Phys. Rev. B: Condens. Matter* **1979**, *20* (8), 3292−3302.
(34) Fowles, G. R. *Introduction to Modern Optics*; Dover Publications: New York, 1968.
(35) Wooten, F. *Optical Properties of Solids*; Academic Press: New York, 1972.

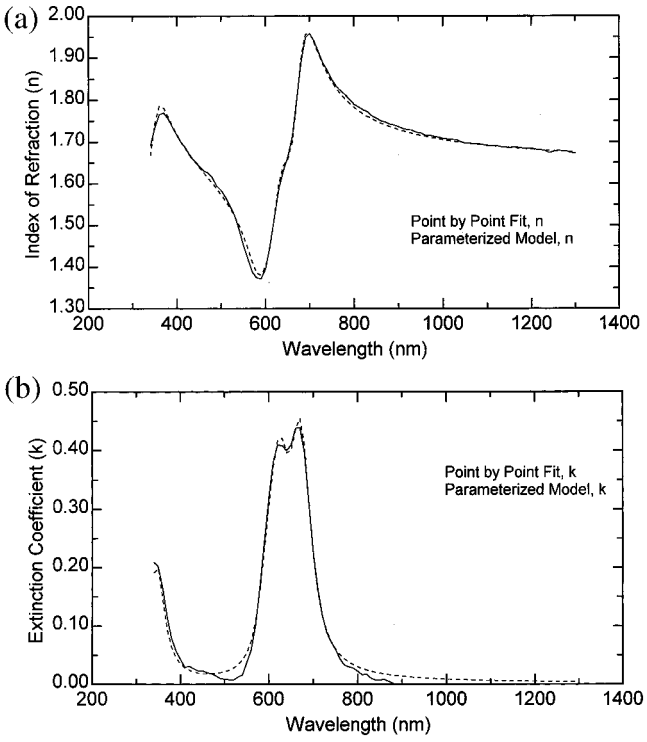

Figure 8. The refractive index *n* (a) and extinction coefficient *k* (b) for the 27 layer-pairs of PDDA−NiPc are derived from experimentally measured Ψ and Δ values based on parametrized models (dashed lines) and direct methods (solid lines). Note that the resonance behavior of the refractive index n corresponds to the absorptions in the extinction coefficient *k* at 630 and 665 nm.

advantage of all dispersion models is that mathematical functions are used to fit for the optical constants at all wavelengths simultaneously, which reduces the sensitivity of *n* and *k* to noisy data.

The refractive index $n(\lambda)$ (Figure 8a) and extinction coefficient $k(\lambda)$ (Figure 8b) were computed as functions of wavelength for the direct method and parametrized models. The refractive index is about $n = 1.6-1.8$ in the nonresonance regions at long wavelength; this agrees well with materials data in the literature.[36] A change in n, typical of resonance, was observed near the absorption regions of 630 and 665 nm. Further, the extinction coefficients deduced from the ellipsometry data predict absorption bands at 630 and 665 nm, in good agreement with the UV−vis absorbance measurement results. The ratio of the two absorption bands, $k(665\text{ nm})/k(630\text{ nm}) = 1.077$ (Figure 8b), measured from ellipsometry of the 27-layer-pair sample at 55, 65, and 75° is in quantitative agreement with the absorbance ratio in the UV−visible spectrum, $A_{665\text{ nm}}/A_{630\text{ nm}} = 1.077$ (Figure 2) for the same sample. The agreement is poorer for the thinner samples, $N = 3$ and 9, perhaps because too little material was available to produce a statistically measurable change in Ψ and Δ. The confidence in the data obtained from spectroscopic ellipsometry improves with film thickness. The improvement is a consequence of the longer path length through thick films, which provides greater sensitivity to the optical constants of the film. For example, the fluctuation in *n* and *k* deduced for the 27-layer-pair sample is negligible for the direct and parametrized methods. The fluctuation increases to 0.02 (rms) for the 9-layer-pair sample and 0.05 (rms) for the 3-layer-pair sample (see Supporting Information).

(36) Musfeldt, J. L.; Tanner, D. B.; Paine, A. J. *J. Opt. Soc. Am. A.* **1993**, *10*, 2648.

Conclusions

With the combination of X-ray reflectometry and spectroscopic ellipsometry, the linear optical constants (*n* and *k*) of self-assembled thin films were determined with a good degree of confidence. The ability to measure linear optical constants from thin films is important because this information is needed in future studies involving the nonlinear optical properties of polymeric materials. These materials are key to the design, fabrication, and optimization of optical devices or modules. For example, controlling refractive index gradient at interfaces is the key to waveguiding in fiber optics and Mach Zender devices. Self-assembly techniques offer tunability of refractive index and coating thickness through layer-by-layer growth of various molecular building blocks. Furthermore, the optical quality, uniformity, and property of the organic thin films are manifested from the quality of these optical parameters. X-ray reflectometry provides an unambiguous measurement of thin-film thickness, which is used to determine optical constants from spectroscopic ellipsometry.

In the present study, NiPc−PDDA layer-pairs grown on silica substrates were measured to be 11(1) Å thick with a surface roughness of 2−7 Å (rms). The refraction index for these films ranged between $n = 1.6$ and $n = 1.8$. Increases in the extinction coefficients determined by spectroscopic ellipsometry were observed at 630 and 665 nm, corresponding well to increases in the absorbance of the films at these wavelengths.

A transition in the growth of PDDA−NiPc layer-pairs on silica substrates, observed as a change in the absorbance of the sample, occurred after about 50 layer-pair depositions. This transition may be related to a transition indicated by a change in surface roughness for PDDA−NiPc layer-pairs grown on a Si substrate, which occurred between 40 and 60 layer-pair depositions.

Acknowledgment. The work of M.L. and M.F. was supported by the U.S. Department of Energy, BES-DMS, under Contract No. W-7405-Eng-36, and the work of D.L. was supported by Laboratory Directed Research and Development.

Supporting Information Available: Figures showing refractive indexes and extinction coefficients for 3 and 9 layer-pairs (5 pages, print/PDF). See any current masthead page for ordering information and web access instructions.

JA981232P